Exploring the mechanisms underlying the phenotype of MCAD deficiency with Systems Medicine

Martines, Anne-Claire

Chapter 7

General discussion

In this thesis, I took a Systems Medicine approach to address the question what elicits hypoketotic hypoglycemia in some MCAD deficient subjects and what protects others against this. In order to do so I evaluated MCAD deficiency in a computational model, in mice in vivo and in humans in vitro. In this chapter I will first discuss the presented projects, the results, implications, follow-up recommendations and future prospects, from computational model to mice to man. Finally, I will end with some overarching conclusions from this thesis.

Navigating from computational metabolic model to mice to man

Computational modeling of mFAO and beyond

In **Chapter 2**, I investigated the origin of the steady-state flux-decline phenomenon observed in the computational model of the isolated mFAO pathway in rat liver. In addition, I investigated the role of enzyme promiscuity in it. I identified that enzyme promiscuity especially that of MCKAT, plays an important role in the flux decline. Enzyme promiscuity leads to inhibition of metabolic reactions by competing substrates. This inhibition appears to result in a strong inhibition of the mFAO flux at cytosolic palmitoyl-CoA concentrations higher than a certain threshold value. Importantly, competitive inhibition and enzyme promiscuity are intricate properties of natural biological processes. It is thus interesting to notice that reactions can reach substantially higher rates in isolation, when a homogeneous substrate mixture is presented to the enzyme, than when the enzyme's properties are changed due to the presence of competing substrates or other modifiers. Persistent imbalances in rates within a network could become detrimental to metabolic homeostasis and cause the development of a pathologic state. I also investigated the sequence of events leading up to the low flux at high palmitoyl-CoA concentrations. I showed that at high cytosolic palmitoyl-CoA concentrations C6 substrate of MCKAT started accumulating substantially before the other intermediates of the pathway. Apparently, MCKAT did not meet the high reaction rates demanded by the large substrate supply, particularly when it was inhibited by all the intermediate acyl-CoA esters. Consequently, a vicious cycle of inhibition by its own substrates and products occurred, resulting in CoASH depletion and lower steady-state fluxes at high cytosolic palmitoyl-CoA concentrations. Interestingly, MCKAT gained positive flux control and CPT1 gained negative flux control at high palmitoyl-CoA concentrations [1]. Typically, the first enzyme in a pathway loses flux control when its substrate concentration increases and the enzyme starts to sense inhibition by its own products or downstream metabolites. Flux control then shifts to enzymes further downstream [2]. The negative flux control exerted by CPT1 at high substrate concentrations distinguished the mFAO model from other pathway structures. In the next section I will evaluate the effects of tacit assumptions in the model, their consequences for the model and a possible way to circumvent them.

Assumptions

As previously indicated, the published models contain several implied assumptions that may be relevant to point out in the light of using these models to make predictions about health and disease. First, I will discuss assumptions on the kinetics of the enzymatic reactions, after which I will deal with assumptions with regard to the metabolites.

Enzymatic reactions proceed in a certain direction when the ΔG is smaller than zero. For enzymatic reactions the Haldane relationship describes the relationship between K_{eq} of the reaction and the reaction-mechanism-specific kinetic parameters. Each reaction mechanism with two or more substrates and products, may have two or more Haldane relations [3]. The mFAO model in its current form is largely based on convenience kinetics [4]. This was a pragmatic choice, since kinetic parameters to describe more complex kinetic mechanisms are scarce. For example, McKean et al. experimentally determined that the acyl-CoA dehydrogenase-catalyzed reaction proceeds according to "Ordered-Bi-Bi" mechanism [5]. One of the corresponding Haldane relationships [3] is

$$e^{\frac{-\Delta G'_0}{RT}} = K_{eq} = \frac{V_f}{V_r} \cdot \frac{K_m^{enoyl-CoA}}{K_i^{acyl-CoA}} \cdot \frac{K_i^{FADH_2}}{K_m^{FAD}}$$

In the mFAO model it was assumed that the K_{eq} of the dehydrogenase reaction was independent of chain-length. Moreover, in the convenience kinetics $KiFADH2$ and $Kiacyl{-}CoA$ do not occur, but $KmFADH2$ and $Kmacyl{-}CoA$do, resulting in the following Haldane relation:

$$K_{eq} = \frac{V_f}{V_r} \cdot \frac{K_m^{enoyl-CoA}}{K_m^{acyl-CoA}} \cdot \frac{K_m^{FADH_2}}{K_m^{FAD}}$$

The question arises to what extent these assumptions change the conclusions drawn from the model. The first assumption that the K_{eq} is chain-length independent might be questionable. Using the online calculator of ΔG_0' and K_{eq} values (eQuilibrator) [6] I calculated that the ratio of K_{eq} values of C_{16}-acyl-CoA dehydrogenation over C_4-acyl-CoA dehydrogenation was less than 0.033. As yet, it is not clear how well and with what error the predictions were made. When correct, however, with the same values for the K_m's the forward V_{max} would be higher relative to the reverse V_{max} when the acyl-CoA chain is shorter. Moreover, some data were available for the K_i's [5]. For acyl-CoA dehydrogenase, for instance, they differed by a factor of 4 from the corresponding K_m's [5]. When I just replace the K_i's by the K_m's I would essentially need to introduce a correction factor (α) in the Haldane equation:

$$K_{eq} = \frac{1}{\alpha} \cdot \frac{V_f}{V_r} \cdot \frac{K_m^{enoyl-CoA}}{K_m^{acyl-CoA}} \cdot \frac{K_m^{FADH_2}}{K_m^{FAD}}$$

More specifically, without the correction factor, the ratio $\frac{V_f}{V_r}$ is 0.38 for the C4-acyl-CoA dehydrogenation reaction, in contrast to a value of 1.52 when the correction factor of 4 was ncluded. In other words, the estimation of the rate at which the reverse reaction runs might be far less in comparison with the forward reaction than used in the original mFAO model. To evaluate this properly, however, the whole 'Ordered Bi Bi equation' should be used. The denominator of the "Ordered Bi Bi" rate equation also contains K_i parameters. This means that the $K_i = K_m$ assumption affects the modeled reaction rate in more than one way [3,7].
In the published mFAO models, cytosolic palmitoyl-CoA was the sole substrate and CPT1 modeled as a strictly C16-specific enzyme [8,9]. When MCA was performed on the published rat model it showed that CPT1 had substantial flux control over the complete range of cytosolic palmitoyl-CoA concentrations [1]. When the C16-specific CPT1 was replaced by a CPT1 with a broad-spectrum chain-length specificity while keeping all other parameters the

same, the strong flux decline at high palmitoyl-CoA concentrations was not present, even with a twice as high CPT1 V_{max} (Figure 1).

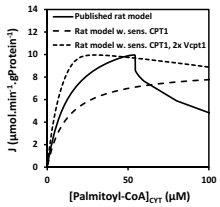

Figure 1. Computational rat dynamic model of isolated mFAO with C16-specific CPT1 (solid lines), with C16-C4 sensitive CPT1 (dashed lines) and with C16-C4 sensitive CPT1 at twice larger V_{max} (short dashed lines).

Although there are no C4-C14 acyl-CoA substrates present in this simulation, the C14-C14 acyl-carnitine products can be formed in the mitochondrial matrix and transported out by CACT. In this way the substrate and product specificity of CPT1 can play a role even in the absence of C4-C14 substrates. This indicates that the chain-length specificity of CPT1 has a strong effect on the mFAO flux, and therefore warrants further study. For instance, in the extended humanized model for MCAD deficiency (**Chapter 5**) accumulating medium-chain acyl-CoA are transported out of the mitochondria as free acids. When these are reactivated to acyl-CoA in the cytosol and transesterified to acyl-carnitine by CPT1, its chain-length specificity becomes important. As shown in **Chapter 5**, a striking difference was observed in the robustness of the mFAO when the chain-length specificity of CPT1 was restricted to palmitoyl-CoA.

Assumptions were also made about the boundary metabolites in the model. Removal, regeneration or reoxidation of several of these compounds were represented by a "sink" reaction. The sink reactions were introduced such that they do not exert any flux control. These are the reoxidation of NADH, conversion of acetyl-CoA back into CoASH and reoxidation of $FADH_2$ that were included as nadhsink, acesink and fadhsink, respectively. However, control of the flux through the mFAO by external effectors *in vivo* is not absent. When these sink reactions would be modelled explicitly, they might share in the total flux control depending on their kinetic parameters and catalytic capacity. This is also in line with the flux control exerted by ETFQO in human model (**Chapter 5**). Thus, the results in **Chapter 2** should be interpreted as the enzymes' share of control for the part of the total flux control that resides in the mFAO pathway itself. Acyl-carnitines were not exported from the cell in the model version used in **Chapter 2** and are therefore technically dead-end metabolites. This represents the experimental conditions of isolated mitochondria in a small reaction vessel, for which the model had been validated [10]. *In vivo*, however, acyl-carnitines can be exported out of the hepatocyte. Export of accumulated acyl equivalents could relieve the modelled system from the consequences of excessive substrate supply. Indeed, introduction of the export of acyl-carnitines, by means of adding simple mass action kinetics ($v=10^{-6}*[C_n\text{-acyl-carnitine}]_{CYT}$), largely resolved the flux-decline phenomenon (Figure 2).

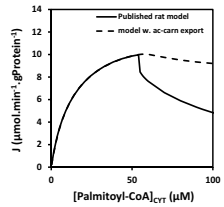

Figure 2. Computational rat dynamic model of isolated mFAO with (dashed lines) and without (solid lines) cytosolic acyl-carnitine export.

Finally, in the model the tacit assumption is made that L-carnitine can never get depleted. Lower plasma L-carnitine levels have however been reported in MCADD individuals [11]. This might bring about lower cytosolic L-carnitine levels. Since carnitine is involved in both the CPT1 and CPT2 catalyzed reactions, changes in carnitine levels might be large enough to have an effect on the CPT-catalyzed reactions. Indeed, as shown in **Chapter 5**, lower L-carnitine levels limit the mFAO flux severely. Thus in reality, cytosolic L-carnitine levels could be considered as part of a regulatory mechanism that keeps CPT1-mediated import of substrate into the mitochondria and oxidation of this substrate in balance. When the mitochondrial oxidation is out of balance with the substrate import, intermediate metabolites accumulate and can be excreted in the urine as their carnitine counterparts. Consequently, carnitine moieties are lost from the cell. If *de novo* synthesis of L-carnitine cannot keep up with the amount of carnitine, L-carnitine levels will decrease. Lower cytosolic acyl-carnitine levels subsequently inhibit the rate of the CPT1-catalyzed reaction and subsequently temporarily decrease the supply of substrate to the mFAO. The mFAO pathway can in turn keep up with the substrate supply of CPT1. The question to be addressed is if this mechanism is quantitatively capable of preventing the flux decline. An alternative scenario would be that the flux decline happens, not because of CoASH depletion but because carnitine levels are so low that CPT1 is severely slowed down. Thus, quantitative analysis of the carnitine economy may have clinical importance.

In **Chapter** 5 I extended the model with a set of enzymatic reaction which can play a role in stabilizing the mFAO. I did not yet study the effects of post-translational modifications (PTMs) on enzyme parameters. Non-enzymatic acylation of mFAO enzymes occurs as the consequence of the very high concentrations of acyl-CoA esters in mitochondria particularly during FAO deficiency. Depending on the metabolic defect enzymes were palmitoylated [12], acetylated, malonylated, succinylated, glutarylated, or butyrylated [13,14]. The effects on enzyme kinetics has not yet been studied in detail. However, recently acylation databases [12,13] have been generated and the ongoing development of tools to predict the effect of these PTMs on kinetic properties [15], resulted very recently in the generation of a database with disease-associated PTMs [16]. These developments may in the near future offer more insight into the effects of PTMs on enzyme kinetic properties in health and disease. I have also not yet considered the role of channeling and submitochondrial localization in the model. As indicated in **Chapter 1 and 2**, all the mFAO enzymes have been shown to associate to OXPHOS supercomplexes and/or other enzymes (including Complex I, HMGCS2, citrate synthase, ETF and ETFQO) that can facilitate the reactions of the corresponding mFAO enzymes. Importantly, it has also been reported that even in C57BL/6 mice, that have an unstable

supercomplex assembly factor 1 (SCAFI), all ETC supercomplexes are at near normal levels and also the respirasome (*i.e* complete assembly of Complex I, III, IV and V) has been found to be at normal levels in the liver, although the reported results are not consistent [17–23]. This suggests condition-dependend supercomplex formation and this should be investigated in MCAD-KO mice.

So, what can be done to improve our understanding of the model's behavior and to improve the accuracy of our dynamic modeling predictions?

The above discussion showed that the assumptions affect the predictions made with the model. It is clear that experimental data on enzyme parameters, where all the actual PTM is included, and metabolite concentrations are needed. Generally, X-Omics technology, including proteomics, metabolomics and lipidomics are promising technologies which might help resolve some of the lack of experimental data. For the humanized model, human precision-cut liver slices are a promising experimental system to mimic human liver [24]. Collaboration with the liver transplantation team in the UMCG offers a unique opportunity to obtain these data. In this section I will further explicitly give some less obvious examples of what can be done to improve our understanding of the model's behavior and the accuracy of the model predictions. If the experimentally-determined reaction mechanism of a reaction is chosen for use in the dynamic model, then the corresponding Haldane relationship can be used to estimate missing product K_m's and K_i's. For example, for the acyl-CoA dehydrogenase reaction, the V_f/V_r ratio is expected to be 3.5 and 7.5 [7,25] and the chain-length-specific K_{eq} between 6 and 180 [6,7,25]. When the K_i and K_m values for FAD and $FADH_2$ are kept the same as in the original model (values originating from [7,26]), the enoyl-CoA K_m's can be estimated. It can subsequently be determined whether using the Haldane relationship in this way for the enzymes in the model has an effect on the model behavior.

Finally, pertaining to experimental validation of dynamic metabolic modeling, preference can be given to results in the first minutes or hour of the simulation. Beyond this, especially in metabolism, the obtained simulation results might become more and more unreliable. This is because in metabolism, processes –with exceptions– can hardly be considered to arrive at a steady state. Metabolic pathways are intricately interconnected, next to the swift and substantial effect that environmental modifiers could have on the functioning of these pathways. It is consequently understandable that in experiments pertaining to metabolism quick action is taken to quench reaction mixtures or freeze-clamp organs to lock a metabolic state until sample analysis. When modeling a metabolic pathway in a dynamic model, where this pathway is often largely isolated, it can take hours before reaching a steady-state. Validation of steady states of such a model might also be essentially unattainable. Substrate concentrations and that of other metabolites and parameters that have been fixed in the model would also have to be maintained constant *in vitro* or *in vivo*. Engineering of experimental setups would be required, like using continuous stirred-tank reactors (CISTRs) and a large amount of living material for a large range of conditions would be needed for the intended validation. In case of isolated mitochondria for instance, substantial functional deterioration can be expected before the required time period necessary to make validation of steady-state results possible. To validate specific steady-state model behaviors, a large number of substrate concentrations need to be tested in a living system, not only to obtain the necessary amount of conditions to make it possible validate steady-state *in silico* results,

but also due to uncertainties in experiments and *in silico* (as indicated above). Therefore, it could be more realistic to simulate conditions that are possible or close to possible in living systems. Herein, it should also be considered what effects external parameters have on the readouts that are intended to validate the *in-silico* results.

Mouse models as tools to understand symptomatology in MCADD

In **Chapter 3**, I investigated which metabolic pathways contribute to the robustness of MCAD-KO mice under fed and fasting conditions on a high- or low-fat diet. Four transcripts of metabolic active enzymes were differentially expressed. Notably, two of the 4 transcripts were from genes encoding for enzymes that catalyze CoA- an NAD(P)(H)-involving reactions. In addition, by means of gene-set-enrichment analyses, I showed that genes coding for enzymes that catalyze CoA- an NAD(P)(H)-involving reactions are altered in expression between WT and KO mice. This is in line with an important role of both cofactors in the computational model of isolated rat mFAO (**Chapter 2**) and of CoA in the MCAD-KO human computational model containing the more C16-specific CPT1 enzyme (**Chapter 5**). Our experimental result from this study are relevant in the context of the "CASTOR" hypothesis by Mitchell *et al*. [27,28]. This hypothesis predicts that CoASH sequestration, toxicity or redistribution (hence CASTOR) would occur in many of impairments in CoA ester degradation pathways, including mFAO deficiencies. It has been proposed [27,28] that many of the typical symptoms presenting in these cases, such as hypoglycemia, are a result of this CASTOR phenomenon. I also observed a downregulation in genes involved in detoxification mechanisms. In line with this, hepatohistological analysis showed a trend towards inflammation in the liver of MCAD-KO mice. Interestingly, in MCAD-KO mouse with the most severe metabolic phenotype after cold exposure (**Chapter 4**), also severe steatohepatitis was observed. This might point to progression of the MCAD-KO phenotype upon switching from exposure to a mild condition to a condition of high-energy demand. The observed liver inflammation might be associated with accumulated ROS, as was reported in human MCADD tissues [29,30]. It is also possible that the robustness in MCAD-KO mice is partly mediated by an adaptation in hepatic mitochondrial content. Analysis of lipid- and protein oxidation and potential adaptation by increased mitochondrial content in the 16-hour fasted mice (**Chapter 3**) are underway.

In **Chapter 4**, where MCAD-KO mice were fasted and subsequently cold-exposed, I obtained three other interesting results. Firstly, I showed for the first time that MCAD-KO mice had significantly lower blood glucose levels at termination than WT mice. In addition, the mouse with the most severe phenotype, showed both severe steatohepatitis and blood glucose decrease during cold exposure, as opposed to the general blood glucose increase observed in both WT and KO mice during cold exposure. With this I have confirmed that the MCAD-KO mouse model, under specific conditions, could be considered a good model for MCAD deficiency in humans. Secondly, I observed a combination of significantly higher blood acyl-carnitine levels, similar hepatic acyl-carnitine levels and higher hepatic levels of medium-chain TG levels in MCAD-KO compared to WT mice. The finding that cold-exposure-induces acyl-carnitine export out of the liver [31,32] together with incorporation of accumulated medium-chain acyl-CoA esters into TGs might help protect MCAD-KO mice against severe liver damage. Thirdly, I observed lower hepatic amino acid levels, but similar blood amino acid levels in MCAD-KO compared to WT mice. As indicated in **Chapter 4**, the hepatic amino

acids might have been used as alternative fuel by the liver, but not to an extent that it would affect blood levels. One may wonder, however, whether other organs that depend on mFAO, would also use more amino acids and why this does not affect the blood concentrations. It would therefore be interesting to measure amino acids in other tissues and possibly also study the turnover of amino acids with stable isotopes [33]. This might give an indication if the systemic amino-acid homeostasis depends on hidden regulation.

In vitro cell models of human MCADD

In **Chapter 6**, I presented a short study, where the levels of acyl-carnitine and select targeted mitochondrial proteins of the energy metabolism were determined in cultured skin fibroblasts of symptomatic and asymtomatic MCADD individuals controls. The fibroblasts of the eldest, asymptomatic MCADD individual showed differences with the other MCADD and healthy control fibroblast, suggesting metabolic adaptations that may relate to the absence of symptoms. Next to this, other cell types could be used to study mechanisms underlying the various phenotypes in MCADD individuals. Promising cell types include patient-derived induced pluripotent stem (iPS) cells which can be differentiated into hepatocytes [34–39]. It will be challenging to develop this into a system that shows a patient-specific liver phenotype. If successful, however, not only a biochemical characterization of the corresponding cells can be performed, but also they can also be used to test the effect of potential treatment strategies on liver metabolism. Examples of potential treatments include the use of the phenylbutyrate, an MCAD-specific xenobiotic substance and drug (Ravicti™), to stabilize the c985A>G mutated protein [40–42], targeting Heat Shock Protein 10 (Hsp10) to increase MCAD protein folding efficiency [43], and supplementation of L-carnitine [44–47] and CoASH precursors [48–52]. Techniques that can be used on the obtained patient materials to better understand the characteristics of symptomatic and asymptomatic MCADD individuals and characteristics of specific MCADD individuals include whole-exome sequencing (to reveal genetic background and potential genetic modifiers), RNA sequencing (to reveal gene-regulation-related adaptations), targeted and shotgun proteomics (to reveal some of the functional adaptations), untargeted metabolomics and fluxomics (the reveal the overall celular metabolic phenotype). These techniques in combination with disease-relevant experimental conditions *in vitro* or *ex vivo* might reveal symptomtology-related genetic and environmental modifiers. The small numbers of patients in combination with the large number of genetic differences that are usually found, will necessitate to combine these classical 'omics technologies with mechanistic modeling.

Next to using patient-derived materials, human hepatic cell lines could be used to understand general mechanisms that affect mFAO when MCAD is deficient. To this end, we have generated an MCAD-KO version of the human hepatocarinoma cell line HepG2, by CRISPR/Cas9 gene editing technique according to [53] (Martines, Vieira Lara, Huijkman, Van de Sluis unpublished). The HepG2 cell line was chosen out of four hepatocarcinoma cell lines, since it had the highest content of proteins involved in the mFAO as determined by targeted proteomics (Figure 3 A).

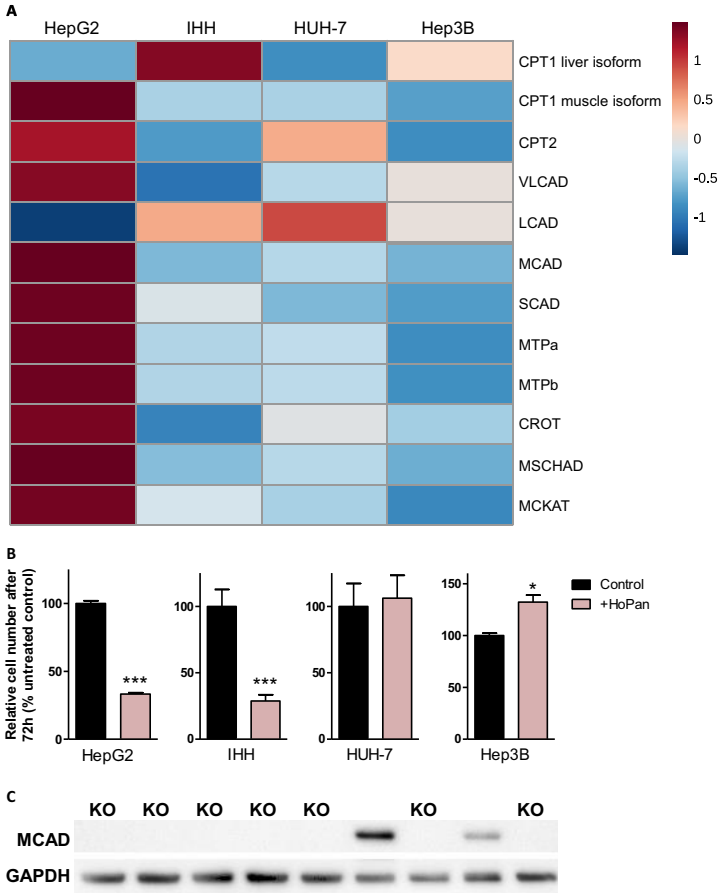

Figure 3. Generation of an MCAD-KO hepatocyte cell line. A: Levels of mFAO proteins in the hepatocarcinoma cell line HepG2, the immortalized human hepatocyte (IHH) and the hepatocarcinoma cell lines HUH-7 and Hep3B (n=1), determined according to [54]. The heatmap was generated with the online tool Metaboanalyst [55]. **B**: Relative cell number after 72h treatment with HoPan vitamin B5-lacking medium. The cells were cultured in the xCELLigence system (Roche Applied Science, Penzberg, Germany; collaboration with Prof. A. Dolga) and cell index values were calculated according to [56]. The cell index values were considered to be proportional to the cell number and used this to estimate the percentage of remaining cells after HoPan treatment. HoPan was a kind gift from Prof. O. Sibon. Results are shown as in bar plots as mean ± SEM, n=3-6 per group, *p<0.05, ***p<0.0001 using unpaired t-test. **C:** Western Blot analysis MCAD protein levels in a selection of HepG2 clones. Glyceraldehyde 3-phosphate dehydrogenase (GAPDH) was used as the household gene. Depicted here is the blot containing the chosen MCAD KO HepG2 (lane 5).

The wild-type HepG2 cell line was also sensitive to the CoASH synthesis inhibitor Hopantenate (HoPan) in medium without the CoASH precursor Vitamin B5 (Figure 3B). This will be relevant to study the interplay between CoASH availability and mFAO. I proceeded with the MCAD-KO HepG2 clone with the cleanest DNA sequence (lane 5 in Figure 3C). When HepG2 cells are cultured in 2% human serum, they resembles primary human hepatocyte more than when they are cultured in 10% fetal calf serum [57–59]. Indeed, upon visual inspection I consistently noticed that the morphology of both the WT and MCAD-KO HepG2

cells started resembling that of primary hepatocytes in the 2% human serum. Moreover, MCAD-KO cultures showed less dividing cells compared to the WT cells (data not shown). The next step will be to analyse biochemically to what extent these cells exhibit a liver-like metabolic phenotype (cf.[60]). Then the MCAD-KO HepG2 cell line will provide a very practical in vitro system to investigate the interplay of the mFAO pathway with surrounding pathways and to validate computer simulations. Examples include the effect of CoASH depletion and low L-carnitine on mFAO flux, glucose production, ketone body production and cell viability in the MCAD-KO compared to the WT HepG2 cells .

Conclusion

This thesis represents a first exploration into MCAD deficiency using a combination of Systems Medicine tools. The work provided insight into the limitations, advantages and disadvantages of computational modeling, *in vivo* experiments in mice and *in vitro* experiments in human material. One of my key overarching findings, both *in silico* and *in vivo*, is the role of Coenzyme A and NAD(P)(H) in mFAO function and MCAD deficiency. The human version of the computational model (**Chapter 5**) offers the opportunity to integrate human data, e.g. from *in vitro* experiments with MCADD patient-specific cells or the new MCAD-KO HepG2 cell line. Thus, I hope that the comprehensive groundwork and discussions laid out in this thesis show promise for future follow-up studies to understand the mechanisms underlying the heterogeneous phenotypes in MCAD deficiency. This should open up new avenues for more personalized diagnoses, prognoses and treatment strategies for MCAD deficiency.

References

1. Martines A-CMF, van Eunen K, Reijngoud D-J, Bakker BM. The promiscuous enzyme medium-chain 3-keto-acyl-CoA thiolase triggers a vicious cycle in fatty-acid beta-oxidation. PLOS Comput Biol. 2017;13(4):1–22.
2. Sauro HM. Correction to “Control and regulation of pathways via negative feedback”. J R Soc Interface. 2017;14(129).
3. CLELAND WW. The kinetics of enzyme-catalyzed reactions with two or more substrates or products. I. Nomenclature and rate equations. Biochim Biophys Acta. 1963 Jan 8;67(2):104–37.
4. Liebermeister W, Klipp E. Bringing metabolic networks to life: Convenience rate law and thermodynamic constraints. Theor Biol Med Model. 2006;3.
5. McKean MC, Frerman FE, Mielke DM. General acyl-CoA dehydrogenase from pig liver. Kinetic and binding studies. J Biol Chem. 1979 Apr 25;254(8):2730–5.
6. Flamholz A, Noor E, Bar-Even A, Milo R. EQuilibrator - The biochemical thermodynamics calculator. Nucleic Acids Res. 2012;40(D1):770–5.
7. Yugi K. Dynamic Kinetic Modeling of Mitochondrial Energy Metabolism. E-Cell Syst Basic Concepts Appl. 2013;105–42.
8. van Eunen K, Simons SMJ, Gerding A, Bleeker A, den Besten G, Touw CML, Houten SM, Groen BK, Krab K, Reijngoud DJ, Bakker BM. Biochemical Competition Makes Fatty-Acid β-Oxidation Vulnerable to Substrate Overload. PLoS Comput Biol. 2013;9(8):2–9.
9. van Eunen K, Volker-Touw CML, Gerding A, Bleeker A, Wolters JC, van Rijt WJ, Martines ACMF, Niezen-Koning KE, Heiner RM, Permentier H, Groen AK, Reijngoud DJ, Derks TGJ, Bakker BM. Living on the edge: Substrate competition explains loss of robustness in mitochondrial fatty-acid oxidation disorders. BMC Biol. 2016;14(1):1–15.
10. van Eunen K, Simons SMJ, Gerding A, Bleeker A, den Besten G, Touw CML, Houten SM, Groen BK, Krab K, Reijngoud DJ, Bakker BM. Biochemical Competition Makes Fatty-Acid β-Oxidation Vulnerable to Substrate Overload. PLoS Comput Biol. 2013;9(8):2–9.
11. Stanley CA, Hale DE, Coates PM, Hall CL, Corkey BE, Yang W, Kelley RI, Gonzales EL, Williamson

JR, Baker L. Medium-chain acyl-CoA dehydrogenase deficiency in children with non-ketotic hypoglycemia and low carnitine levels. Pediatr Res. 1983;17(11):877–84.
12. Blanc M, David F, Abrami L, Migliozzi D, Armand F, Bürgi J, van der Goot FG. SwissPalm: Protein Palmitoylation database. F1000Research. 2015;4(0):261.
13. Xu H, Zhou J, Lin S, Deng W, Zhang Y, Xue Y. PLMD: An updated data resource of protein lysine modifications. J Genet Genomics. 2017 May 20;44(5):243–50.
14. Pougovkina O, te Brinke H, Wanders RJA, Houten SM, de Boer VCJ. Aberrant protein acylation is a common observation in inborn errors of acyl-CoA metabolism. J Inherit Metab Dis. 2014;37(5):709–14.
15. Audagnotto M, Dal Peraro M. Protein post-translational modifications: In silico prediction tools and molecular modeling. Comput Struct Biotechnol J. 2017;15:307–19.
16. Xu H, Wang Y, Lin S, Deng W, Peng D, Cui Q, Xue Y. PTMD: A Database of Human Disease-associated Post-translational Modifications. Genomics Proteomics Bioinformatics. 2018;16(4):244–51.
17. Lapuente-Brun E, Moreno-Loshuertos R, Acin-Perez R, Latorre-Pellicer A, Colas C, Balsa E, Perales-Clemente E, Quiros PM, Calvo E, Rodriguez-Hernandez MA, Navas P, Cruz R, Carracedo A, Lopez-Otin C, Perez-Martos A, Fernandez-Silva P, Fernandez-Vizarra E, Enriquez JA. Supercomplex Assembly Determines Electron Flux in the Mitochondrial Electron Transport Chain. Science (80-). 2013;340(6140):1567–70.
18. Jha P, Wang X, Auwerx J. Analysis of Mitochondrial Respiratory Chain Supercomplexes Using Blue Native Polyacrylamide Gel Electrophoresis (BN-PAGE). Curr Protoc Mouse Biol. 2016;6(1):1–14.
19. Cogliati S, Calvo E, Loureiro M, Guaras AM, Nieto-Arellano R, Garcia-Poyatos C, Ezkurdia I, Mercader N, Vázquez J, Enriquez JA. Mechanism of super-assembly of respiratory complexes III and IV. Nature. 2016;539(7630):579–82.
20. Mourier A, Matic S, Ruzzenente B, Larsson N-G, Milenkovic D. The respiratory chain supercomplex organization is independent of COX7a2l isoforms. Cell Metab. 2014 Dec 2;20(6):1069–75.
21. Williams EG, Wu Y, Jha P, Dubuis S, Blattmann P, Argmann CA, Houten SM, Amariuta T, Wolski W, Zamboni N, Aebersold R, Auwerx J. Systems proteomics of liver mitochondria function. Science. 2016 Jun 10;352(6291):aad0189.
22. Shiba S, Ikeda K, Horie-Inoue K, Nakayama A, Tanaka T, Inoue S. Deficiency of COX7RP, a mitochondrial supercomplex assembly promoting factor, lowers blood glucose level in mice. Sci Rep. 2017;7(1):7606.
23. Milenkovic D, Blaza JN, Larsson NG, Hirst J. The Enigma of the Respiratory Chain Supercomplex. Cell Metab. 2017;25(4):765–76.
24. Vatakuti S, Olinga P, Pennings JLA, Groothuis GMM. Validation of precision-cut liver slices to study drug-induced cholestasis: a transcriptomics approach. Arch Toxicol. 2017;91(3):1401–12.
25. Kohn MC, Garfinkel D. Computer simulation of metabolism in palmitate-perfused rat heart. I. Palmitate oxidation. Ann Biomed Eng. 1983;11(5):361–84.
26. Yugi K, Tomita M. A general computational model of mitochondrial metabolism in a whole organelle scale. Bioinformatics. 2004;20(11):1795–6.
27. Mitchell GA, Gauthier N, Lesimple A, Wang SP, Mamer O, Qureshi I. Hereditary and acquired diseases of acyl-coenzyme A metabolism. Mol Genet Metab. 2008;94(1):4–15.
28. Yang H, Zhao C, Wang Y, Wang SP, Mitchell GA. Hereditary diseases of coenzyme A thioester metabolism. Biochem Soc Trans. 2019 Feb 28;47(1):149–55.
29. Lim SC, Tajika M, Shimura M, Carey KT, Stroud DA, Murayama K, Ohtake A, McKenzie M. Loss of the Mitochondrial Fatty Acid β-Oxidation Protein Medium-Chain Acyl-Coenzyme A Dehydrogenase Disrupts Oxidative Phosphorylation Protein Complex Stability and Function. Sci Rep. 2018;8(1):1–17.
30. Derks TGJ, Touw CML, Ribas GS, Biancini GB, Vanzin CS, Negretto G, Mescka CP, Reijngoud DJ, Smit GPA, Wajner M, Vargas CR. Experimental evidence for protein oxidative damage and altered antioxidant defense in patients with medium-chain acyl-CoA dehydrogenase deficiency. J Inherit Metab Dis. 2014;37(5):783–9.
31. Simcox J, Geoghegan G, Maschek JA, Bensard CL, Pasquali M, Miao R, Lee S, Jiang L, Huck I,

Kershaw EE, Donato AJ, Apte U, Longo N, Rutter J, Schreiber R, Zechner R, Cox J, Villanueva CJ. Global Analysis of Plasma Lipids Identifies Liver-Derived Acylcarnitines as a Fuel Source for Brown Fat Thermogenesis. Cell Metab. 2017;26(3):509–522.e6.
32. Abumrad NA. The Liver as a Hub in Thermogenesis. Cell Metab. 2017;26(3):454–5.
33. Hui S, Ghergurovich JM, Morscher RJ, Jang C, Teng X, Lu W, Esparza LA, Reya T, Le Zhan, Yanxiang Guo J, White E, Rabinowitz JD. Glucose feeds the TCA cycle via circulating lactate. Nature. 2017;551(7678):115–8.
34. Kumar S, Blangero J, Curran JE. Induced pluripotent stem cells in disease modeling and gene identification. Methods Mol Biol. 2018;1706:17–38.
35. Dutta D, Heo I, Clevers H. Disease Modeling in Stem Cell-Derived 3D Organoid Systems. Trends Mol Med. 2017;23(5):393–410.
36. Huch M, Knoblich JA, Lutolf MP, Martinez-Arias A. The hope and the hype of organoid research. Development. 2017;144(6):938–41.
37. Yang H, Sun L, Liu M, Mao Y. Patient-derived organoids: a promising model for personalized cancer treatment. Gastroenterol Rep. 2018;6(4):243–5.
38. Haddrick M, Simpson PB. Organ-on-a-chip technology: turningt its potential for clinical benefit into reality. Drug Discov Today. 2019;00(00).
39. Beckwitt CH, Clark AM, Wheeler S, Taylor DL, Stolz DB, Griffith L, Wells A. Liver 'organ on a chip.' Exp Cell Res. 2018;363(1):15–25.
40. Kang H. Exploring therapeutic approaches for treatment of medium-chain acyl-CoA dehydrogenase (MCAD) deficiency. 2014.
41. Vockley G. Use of Ravicti™ in Patients With MCAD Deficiency With the 985A>G (K304E) Mutation [Internet]. 2017 [cited 2019 Apr 21]. Available from: https://clinicaltrials.gov/ct2/show/study/NCT01881984
42. Palir N, Ruiter JPN, Wanders RJA, Houtkooper RH. Identification of enzymes involved in oxidation of phenylbutyrate. J Lipid Res. 2017;58(5):955–61.
43. Lu Z, Chen Y, Aponte AM, Battaglia V, Gucek M, Sack MN. Prolonged fasting identifies heat shock protein 10 as a sirtuin 3 substrate: Elucidating a new mechanism linking mitochondrial protein acetylation to fatty acid oxidation enzyme folding and function. J Biol Chem. 2015;290(4):2466–76.
44. Bakermans AJ, Van Weeghel M, Denis S, Nicolay K, Prompers JJ, Houten SM. Carnitine supplementation attenuates myocardial lipid accumulation in long-chain acyl-CoA dehydrogenase knockout mice. J Inherit Metab Dis. 2013;36(6):973–81.
45. Bene J, Hadzsiev K, Melegh B. Role of carnitine and its derivatives in the development and management of type 2 diabetes. Nutr Diabetes. 2018;8(1):1–10.
46. Spiekerkoetter U, Bastin J, Gillingham M, Morris A, Wijburg F, Wilcken B. Current issues regarding treatment of mitochondrial fatty acid oxidation disorders. J Inherit Metab Dis. 2010;33(5):555–61.
47. Walter JH. L-Carnitine in inborn errors of metabolism: What is the evidence? J Inherit Metab Dis. 2003;26(2–3):181–8.
48. Srinivasan B, Baratashvili M, Zwaag M Van Der, Kanon B, Colombelli C, Schaap O, Nollen EAA, Podgoršek A, Kosec G, Petkovi H, Hayflick S. Extracellular 4 ' -Phosphopantetheine is a source for intracellular Coenzyme A synthesis. Nat Chem Biol. 2015;11(August):1–26.
49. Sharma LK, Subramanian C, Yun MK, Frank MW, White SW, Rock CO, Lee RE, Jackowski S. A therapeutic approach to pantothenate kinase associated neurodegeneration. Nat Commun. 2018;9(1).
50. Di Meo I, Colombelli C, Srinivasan B, de Villiers M, Hamada J, Jeong SY, Fox R, Woltjer RL, Tepper PG, Lahaye LL, Rizzetto E, Harrs CH, de Boer T, van der Zwaag M, Jenko B, Čusak A, Pahor J, Kosec G, Grzeschik NA, Hayflick SJ, Tiranti V, Sibon OCM. Acetyl-4'-phosphopantetheine is stable in serum and prevents phenotypes induced by pantothenate kinase deficiency. Sci Rep. 2017 Sep 12;7(1):11260.
51. Mitchell GA, Gauthier N, Lesimple A, Wang SP, Mamer O, Qureshi I. Hereditary and acquired diseases of acyl-coenzyme A metabolism. Mol Genet Metab. 2008;94(1):4–15.
52. Yang H, Zhao C, Wang Y, Wang SP, Mitchell GA. Hereditary diseases of coenzyme A thioester metabolism. Biochem Soc Trans. 2019;47(1):149–55.
53. Ran FA, Hsu PD, Wright J, Agarwala V, Scott DA, Zhang F. Genome engineering using the CRISPR-

Cas9 system. Nat Protoc. 2013;8(11):2281–308.
54. Wolters JC, Ciapaite J, Van Eunen K, Niezen-Koning KE, Matton A, Porte RJ, Horvatovich P, Bakker BM, Bischoff R, Permentier HP. Translational Targeted Proteomics Profiling of Mitochondrial Energy Metabolic Pathways in Mouse and Human Samples. J Proteome Res. 2016;15(9):3204–13.
55. Xia J, Psychogios N, Young N, Wishart DS. MetaboAnalyst : a web server for metabolomic data analysis and interpretation. 2009;37(May):652–60.
56. Diemert S, Dolga AM, Tobaben S, Grohm J, Pfeifer S, Oexler E, Culmsee C. Impedance measurement for real time detection of neuronal cell death. J Neurosci Methods. 2012 Jan 15;203(1):69–77.
57. Gunn PJ, Green CJ, Pramfalk C, Hodson L. In vitro cellular models of human hepatic fatty acid metabolism: Differences between Huh7 and HepG2 cell lines in human and fetal bovine culturing serum. Physiol Rep. 2017;5(24):1–12.
58. Steenbergen R, Oti M, Ter Horst R, Tat W, Neufeldt C, Belovodskiy A, Chua TT, Cho WJ, Joyce M, Dutilh BE, Tyrrell DL. Establishing normal metabolism and differentiation in hepatocellular carcinoma cells by culturing in adult human serum. Sci Rep. 2018 Aug 3;8(1):11685.
59. Pramfalk C, Larsson L, Härdfeldt J, Eriksson M, Parini P. Culturing of HepG2 cells with human serum improve their functionality and suitability in studies of lipid metabolism. Biochim Biophys Acta - Mol Cell Biol Lipids. 2016;1861(1):51–9.
60. Samanez CH, Caron S, Briand O, Dehondt H, Duplan I, Kuipers F, Hennuyer N, Clavey V, Staels B. The human hepatocyte cell lines IHH and HepaRG: models to study glucose, lipid and lipoprotein metabolism. Arch Physiol Biochem. 2012;118(March):102–11.

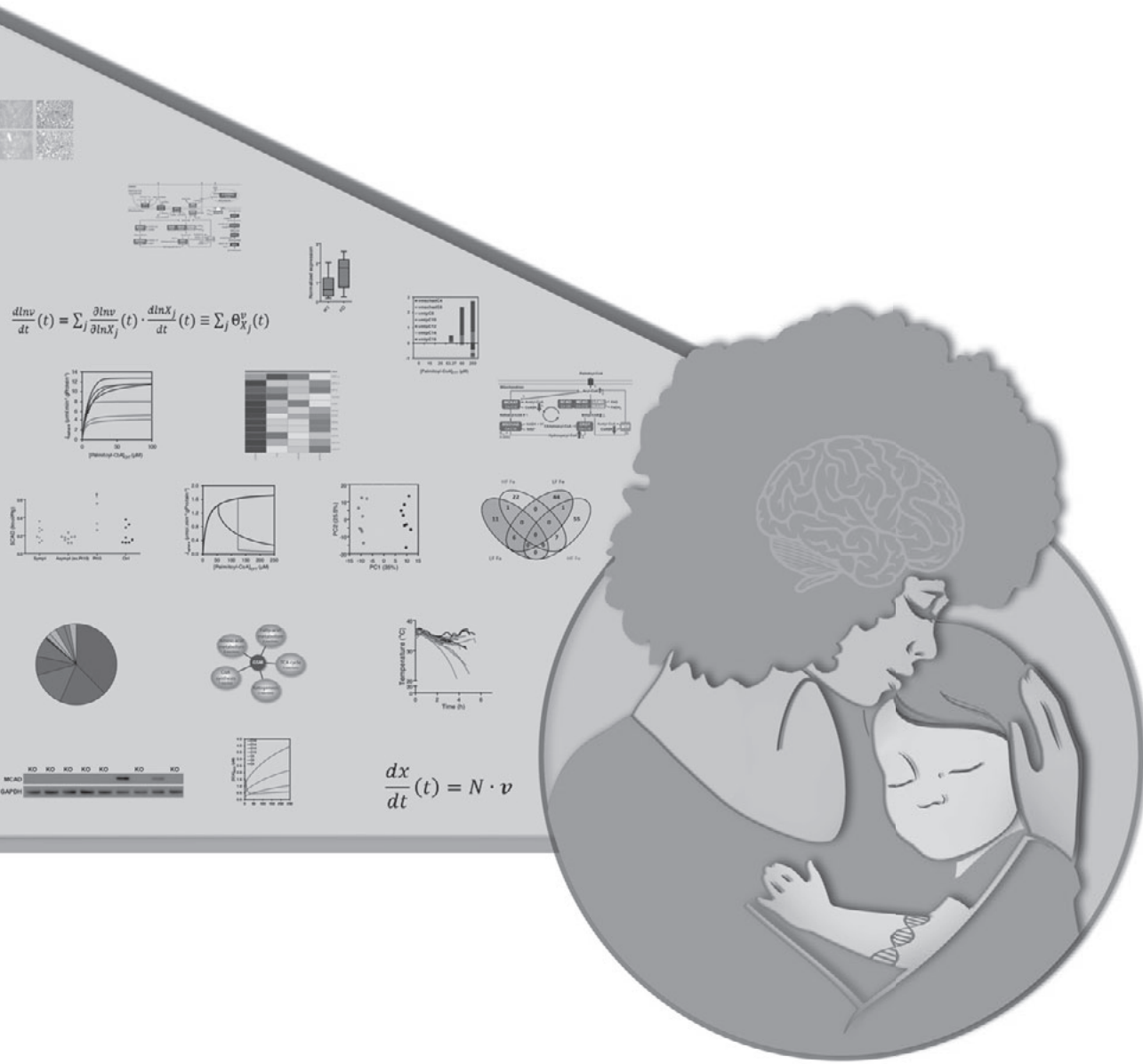
$\frac{dlnv}{dt}(t) = \sum_j \frac{\partial lnv}{\partial lnX_j}(t) \cdot \frac{dlnX_j}{dt}(t) \equiv \sum_j \theta^v_{X_j}(t)$
KO KO KO KO KO KO KO
MCAD
GAPDH
$\frac{dx}{dt}(t) = N \cdot v$